

1 Supplementary file

2 **Distribution fitting procedure**

3 Clauset et al. (2009) and Rizzo et al (2017) proposed that the maximum likelihood estimator (MLE)
4 should be preferred over use of least square regression analyses (R^2) for the fitting of power-law
5 distributions. Rizzo et al. (2017) performed the MLE on power-law, log-normal and exponential
6 distributions by using a suite of custom MATLAB™ functions, integrated into FracPaQ (Healy et al.,
7 2017). The MLE approach maximizes the likelihood, gives estimate of the governing parameters (α
8 for power-law distribution, λ for exponential distribution and μ and σ for the log-normal distribution)
9 of the different fitting equations:

$$\text{Power-law: } p(x|\alpha) = \frac{\alpha-1}{x_{\min}} \left(\frac{x}{x_{\min}} \right)^{-\alpha} \quad \text{Eq. 1}$$

$$\text{Log-normal: } p(x|\mu, \sigma) = \frac{1}{x\sigma\sqrt{2\pi}} \exp\left(-\frac{(\ln x - \mu)^2}{2\sigma^2}\right) \quad \text{Eq. 2}$$

$$\text{Exponential: } p(x|\lambda) = \lambda \exp(-\lambda x) \quad \text{Eq. 3}$$

10

11 where x_{\min} in the power-law distribution, is a required parameter representing the lower bound
12 below which the power-law distribution is not valid (Clauset et al., 2009). The x_{\min} parameter can be
13 estimated using the Kolmogorov-Smirnov (KS) test which minimizes the difference between the data
14 and the synthetic data generated using the parameters derived from the MLE (Clauset et al., 2009;
15 Rizzo et al., 2017). The K-S test generates an H-percentage (HP) which is the probability of accepting
16 the H0 (null hypothesis) result over the total n -cycles (in this case $n = 2500$). If the p -value is less
17 than or equal to 0.05, the test suggests that “the observed data are inconsistent with the null
18 hypothesis, so the null hypothesis must be rejected, while if the p -value is far from zero and close to
19 1, the observed data are not inconsistent with the null hypothesis, and the chosen fitting method
20 can be applied” (Light et al., 2009). However having a p -value larger than 0.05, does not prove that
21 the tested hypothesis is the most appropriate distribution. Clauset et al. (2009) suggest that the p -
22 value for alternative distributions can be calculated to test between other possible distributions. We

23 used the KS probability value (reported in tables S2 & S2) to decide between log normal and power
24 law distributions. In almost all examples, the exponential fit yielded a noticeably poorer result so is
25 discounted.

26

27 Knowing that attributes collected from outcrop are naturally affected by truncation and
28 censoring bias, we also performed the MLE and KS test for truncated populations defined by
29 step-wise removal of data values from either end of the distribution (Fig. S1). We term these
30 the upper cut (uc) and lower cut (lc) respectively. 40 values of censoring and truncation for
31 uc and lc were considered, resulting in 800 simulations. The resulting values of KS values were
32 visualized a checkerboard-like plots (e.g. Fig S1). The best-fit results produce the highest
33 percentage values red colours in Fig 5.

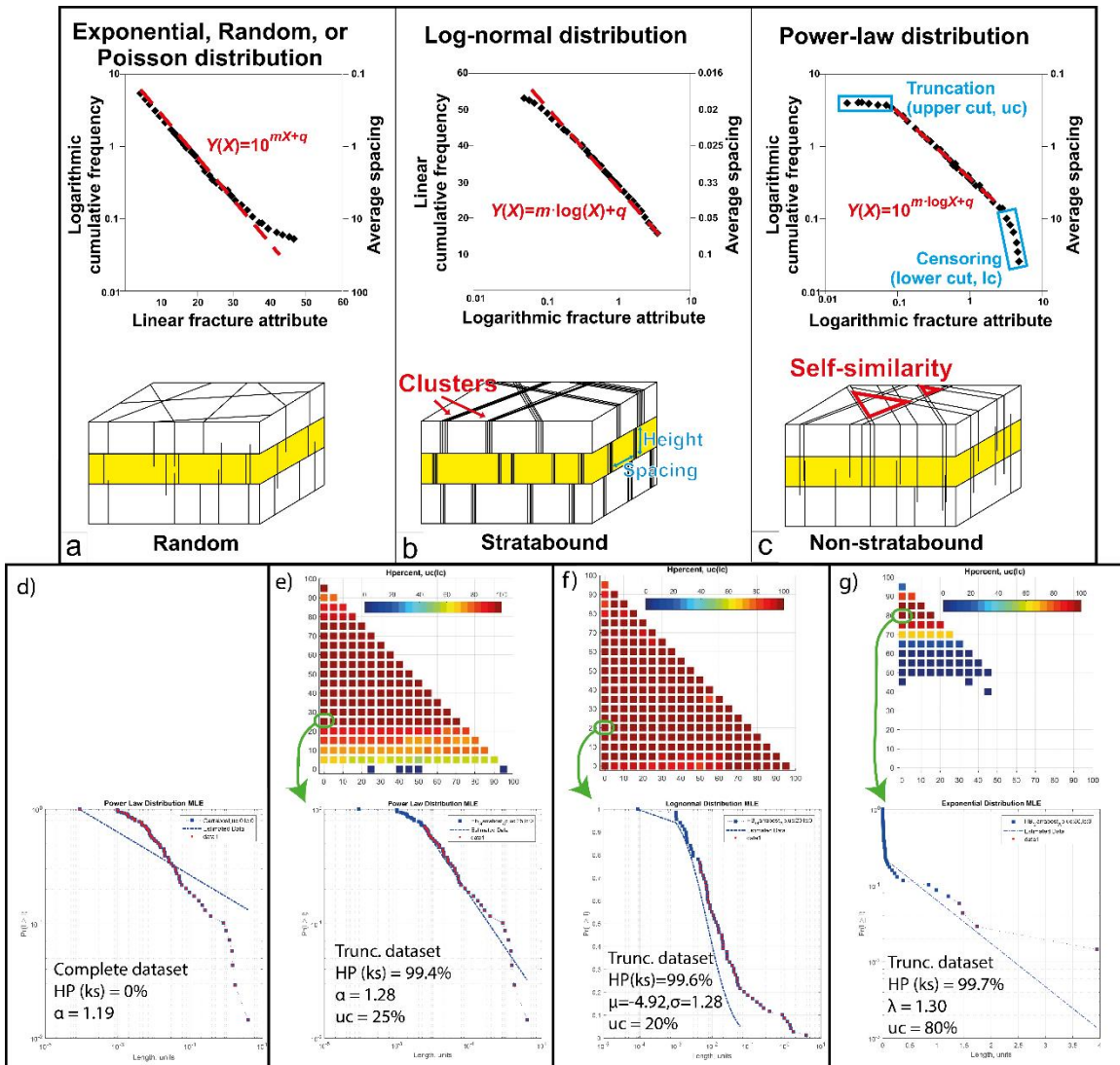
34

35 In Table S1 and S2 we report the KS value (HP), and distribution coefficients obtained using
36 the MLE for both non-truncated (power-law distributions) and for truncated (power-law
37 distribution, exponential and log normal) populations aperture and length.

38

39 Complete (non-truncated) populations are generally best described by a log-normal
40 distribution (they show consistently high percentage fitting values). However, the KS values
41 for truncated log-normal and truncated power-law datasets are similar suggesting either
42 distribution might be preferred. The choice of the best-fit distribution should not be based on
43 complete population because population “end-points” (blue regions in Fig S1) are biased. For
44 the datasets the aperture data can mostly be well describe by power-law distribution whereas
45 the length data could be described by either power-law or log normal distributions.

46



47

48 Fig S1. Example fracture distributions and models that show their typical development (after Dichiarante et al In
49 Review) a) An exponential or random distribution, b) a log-normal distribution producing fracture corridors and
50 c) a scale invariant power law distribution. d) an example of the modified Rizzo et al (2017) MLE distribution
51 fitting procedure for a basement outcrop dataset from Garrabost, Hebrides. Complete dataset shows a poor
52 power law fit, e) same dataset with a truncated (25%) picked as the minimum value of uc/lc from checkerboard
53 of KS results that gives a good fit (>99% Ks value – dark red colour). f) the log-normal result for same dataset
54 and g) the exponential result. All of the these fits are acceptable, however the exponential can be dismissed as
55 80% of the data have been removed from the analysis, the power law and log normal are very close with a slight
56 preference for the log normal distribution (slightly higher KS value and slightly more of the data included).

Table S1 - Fracture Aperture data - distribution fitting parameters

Dataset Grid Reference Transect	Mainland Lewisian												Mainland Lewisian (contd)											
	AnB002	Assynt3 L1	Assynt ft	Assynt Shore_L1	CaolasCum	Clachtoll	Gruinard2	Gruinard	KLB_10	KLB_1	KLB_2	KLB_L1	Lagg_Fish	Loch Inver	OSM	Shegra2	Shegra	Skerricha	TACperP2	TACperP	TTr2A			
	NC 0508 2624	NC 2006 2582	NC 2101 2510	NC 2028 2559	NC 2251 3392	NC 0425 2677	NG 8625 9097	NG 8625 9097	NC 2296 5621	NC 2296 5621	NC 2296 5621	NC 2296 5621	NC 0835 3097	NC 1000 2357	NC 2010 5832	NC 1804 6027	NC 1801 6004	NC 2462 5100	NC 4510 6577	NC 4510 6577	NC 4510 6577			
Orientation	102	242	139	158	53	169	152	152	167	280	316	280	135	228	58	307	93	141	62	266	350			
	Banded grey, medium grained orthogneisses	High grade intermediate to mafic orthogneisses	High grade intermediate to mafic orthogneisses	High grade intermediate to mafic orthogneisses	Grey ooid orthogneisses (intermediate to mafic), Canisp Shear fabrics	Granulite facies TTG gneisses	Granulite facies TTG gneisses	Granulite facies TTG gneisses	Light to dark grey diorite/granodiorite gneiss, with younger mafic pods. Granite and pegmatite intrusions	Light to dark grey diorite/granodiorite gneiss, with younger mafic pods. Granite and pegmatite intrusions	Light to dark grey diorite/granodiorite gneiss, with younger mafic pods. Granite and pegmatite intrusions	Amphibolite-grade banded grey quartz diorite/granodiorite gneisse, banded in places with younger mafic pods. Granite and pegmatite intrusions	Light to dark grey diorite/granodiorite gneiss, banded in places with younger mafic pods. Granite and pegmatite intrusions	Light to dark grey diorite/granodiorite gneiss, banded in places with younger mafic pods. Granite and pegmatite intrusions	Light to dark grey diorite/granodiorite gneiss, banded in places with younger mafic pods. Granite and pegmatite intrusions	Light to dark grey diorite/granodiorite gneiss, banded in places with younger mafic pods. Granite and pegmatite intrusions	Light to dark grey diorite/granodiorite gneiss, banded in places with younger mafic pods. Granite and pegmatite intrusions	Light to dark grey diorite/granodiorite gneiss, banded in places with younger mafic pods. Granite and pegmatite intrusions	Light to dark grey diorite/granodiorite gneiss, banded in places with younger mafic pods. Granite and pegmatite intrusions	Light to dark grey diorite/granodiorite gneiss, banded in places with younger mafic pods. Granite and pegmatite intrusions	Light to dark grey diorite/granodiorite gneiss, banded in places with younger mafic pods. Granite and pegmatite intrusions	Light to dark grey diorite/granodiorite gneiss, banded in places with younger mafic pods. Granite and pegmatite intrusions		
Lithology	Assynt terrane, Canisp Shear zone margin	Assynt terrane, background gneiss fabrics	Assynt terrane, background gneiss fabrics	Assynt terrane, background gneiss fabrics	Assynt terrane, little pre-existing structure	Rhiconich terrane, Canisp Shear zone margin	Gairloch shear zone fabrics	Gairloch shear zone fabrics	Rhiconich terrane, close to Kinlochbervie fault	Rhiconich terrane, close to Kinlochbervie fault	Rhiconich terrane, close to Kinlochbervie fault	Assynt terrane, background gneiss fabrics	Assynt terrane, background gneiss fabrics	Rhiconich terrane, background gneiss fabrics	Rhiconich terrane, background gneiss fabrics	Rhiconich terrane, background gneiss fabrics	Rhiconich Terrane, perpendicular to foliation	Rhiconich Terrane, parallel to foliation	Rhiconich Terrane, parallel to foliation					
	208	53	50	42	50	65	76	76	81	94	61	81	47	72	53	83	51	77	107	57	43			
Structure Number of fractures	12,728	8	3.25	6	113	14.5	50	15	20	35	30	30	9	20	13	30	20	40	30	20	20			
	Power law fit for entire sample																							
PL Prob	0	78.08	0.12	96.8	0	34.96	0	0	12.48	12.48	5.52	80.76	0	3	87.88	0	0	0.08	0	0	68.08			
	PL α	1.47	2.03	1.37	2.07	1.45	1.42	1.45	1.59	1.68	1.56	1.93	1.88	1.67	1.50	1.44	1.62	1.52	1.43	1.45	1.96			
	uc	0	0	0	0	0	0	0	0	0	0	0	0	0	0	0	0	0	0	0	0	0	0	
	lc	0	0	0	0	0	0	0	0	0	0	0	0	0	0	0	0	0	0	0	0	0	0	
Truncated and censored sample distribution fitting using MLE approach (see text)																								
LN Prob	98.92	99.2	99.36	99.44	98.12	98.4	96	96.44	98.96	98.04	98.64	83	99.84	99.52	99.72	99.72	98.28	99.84	99.64	99.24	99.88			
	LN mu	-1.41	-0.45	-0.51	-0.14	-5.78	-5.47	-4.98	-5.46	-4.53	-3.95	-5.52	-0.11	-57916.00	-6.07	-3.44	-4.95	-8.63	-6.03	-4.57	-0.66			
	LN sigma	0.30	0.22	0.72	0.55	0.25	0.81	0.73	1.10	1.09	2.33	0.49	0.83	0.33	0.75	0.83	0.91	0.43	0.66	0.27	0.43	0.30		
	uc	25	65	0	0	10	15	0	0	0	0	10	0	15	30	5	0	10	80	15	5	30		
	lc	20	0	0	0	85	25	90	70	80	75	50	0	65	50	75	75	65	15	75	70	15		
Exp prob	0.04	24.08	52.92	0.80	97.64	99.60	83.80	97.36	0.00	0.00	4.72	24.64	94.88	85.36	99.64	74.76	0.00	71.44	97.20	97.28	14.96			
	Lambda	2.75	1.58	1.39	541.97	89.55	6.38	128.21	97.56	148.62	71.73	153.65	0.83	104.00	36.36	15.79	100.78	190.48	90.00	20.20	1.87			
	uc	0	0	0	0	95	95	85	0	0	0	0	75	0	75	85	100	95	85	0	0			
	lc	55	10	60	20	0	0	0	0	0	0	0	0	10	0	5	0	0	5	0	45			
PL Prob T&C	98.84	98.12	99.56	98.56	99.96	99.48	97.88	99.4	97.44	98.72	98.8	99.72	99.84	99.48	99.84	99.92	96.16	99.8	99.88	99.76	99.84			
	PL α	2.36	3.22	3.21	2.32	1.93	1.81	2.81	2.06	2.01	1.75	2.11	2.03	2.15	1.81	1.66	2.00	1.64	2.54	2.08	3.37			
	xmin	0.23	1.45	0.63	0.74	0.005	0.002	0.003	0.004	0.004	0.004	0.003	0.037	0.002	0.006	0.007	0.001	0.007	0.004	0.01	0.83			
	uc	40	65	45	35	95	40	90	85	85	75	60	5	65	87.5	70	90	55	95	85	65			
	lc	0	0	5	2	0	0	0	1	0	0	1	0	10	0	0	20	0	0	5	0			

Clair											
Aperture Grid Reference	JP2067a_2 n/a	JP2067a_2core3 n/a	JP2067a_2core4 n/a	JP2067a_2core5 n/a	JP2067a_2core6 n/a	JP2067a_2core8 n/a	JP2067a_2core9 n/a	JP2068_8 n/a	KM2067a_2core3 n/a	KM2067a_2core4 n/a	KM2067a_2core8 n/a
Transect Orientation	horizontal	horizontal	horizontal	horizontal	horizontal	horizontal	horizontal	horizontal	horizontal	horizontal	horizontal
Lithology	Banded gneiss	Banded gneiss	Banded gneiss	Banded gneiss	Banded gneiss	Banded gneiss	Banded gneiss	Banded gneiss	Banded gneiss	Banded gneiss	Banded gneiss
Structure Number of fractures	Fractured gneiss	Fractured gneiss	Fractured gneiss	Fractured gneiss	Fractured gneiss	Fractured gneiss	Fractured gneiss	Fractured gneiss	Fractured gneiss	Fractured gneiss	Fractured gneiss
Length (m)	78	45	34	36	20	23	22	33	132	131	45
	10	10	10	10	10	10	10	10	10	10	10
Power law fit for entire sample											
PL Prob	1.8	50.28	82.12	47.8	97.96	76.48	86.04	86.68	0	0	65.4
PL α	1.31	1.32	1.42	1.31	1.41	1.35	1.33	1.37	1.25	1.24	1.3
uc	0	0	0	0	0	0	0	0	0	0	0
lc	0	0	0	0	0	0	0	0	0	0	0
Truncated and censored sample distribution fitting Using MLE approach (see text)											
LN Prob	99.6	99.64	99.6	98.56	100	99.6	99.48	99.68	99.24	99.36	99.7
LN mu	-5.3	-5.588	-5.88	-6.1	-6.8735	-6.491	-6.31	-5.87	-7.92	-7.19	-5.59
LN sigma	1.38	1.577	1.33	1.39	0.91	1.32	1.49	1.45	0.71	0.8001	1.58
uc	0	0	0	0	30	0	0	0	35	20	0
lc	0	0	0	0	0	0	0	0	20	20	0
Exp prob											
Lambda	94.68	97.96	96.84	96.8	99.4	98.44	88.76	96.4	97.08	81.76	97.6
uc	90.93	75.89	154.92	91.52	87.71	300.43	181	119.68	97.07	346.34	75.85
lc	5	25	10	60	30	10	10	20	85	40	25
PL Prob T&C											
PL α	1.88	1.97	1.74	1.61	1.58	1.52	1.56	1.54	1.892	2.16	1.52
xmin	0.0047	0.0065	0.019	0.0007	0.0007	0.0003	0.0006	0.0008	0.0007	0.003	0.001
uc	45	60	35	15	30	10	20	20	55	85	20
lc	5	10	8	6	5	5	10	10	5	8	10

Table S2 Fracture length attributes - distribution fitting parameters

Mainland Lewisan																		
ID Length (PL1)	ML_AchmelvichBeach_L1	ML_ArB3_L1	ML_ArB6_L1	ML_ArB8_L1	ML_ArBTT002_L1	ML_Asynct3_L1	ML_Asynctt_L1	ML_Asynthore_L1	ML_Clauchtoll_L1	ML_CS22_L1	ML_CS23_L1	ML_KLB_L1	ML_LochAsynct2_L1	ML_LochAsynct3_L1	ML_Oldshoremore1_L1	ML_Rispond_L1	ML_TraighAlltChallenge_L1	ML_Tra2_L1
Dataset	Achmelvich	Altan na bradhan	Altan na bradhan	Altan na bradhan	Altan na bradhan	Assint	Assint, fieldtrip location	AssintShore_L1	Clauchtoll	Canisp SZ	Canisp SZ	Kinlochbervie	Loch Asynct Shore	Oldshoremore	Rispond	Traig Alt Challenge	Traig Alt Challenge	
Grid Reference	NC 0566 2498	NC 0508 2624	NC 0508 2624	NC 0508 2624	NC 0508 2624	NC 2006 2582	NC 2101 2510	NC 2028 2559	NC 0425 2677	NC 0528 2581	NC 0581 2559	NC 2296 5621	NC 2028 2559	NC 2010 5832	NC 4508 6557	NC 4510 6577	NC 4510 6577	
Transect Orientation	230	102	102	102	102	139	158	169	281	281	281	280	158	242	58	62	266	
Lithology	High grade intermediate to mafic orthogneisses	Banded grey, medium grained orthogneisses	Banded grey, medium grained orthogneisses	Banded grey, medium grained orthogneisses	Banded grey, medium grained orthogneisses	High grade intermediate to mafic orthogneisses	High grade intermediate to mafic orthogneisses	High grade intermediate to mafic orthogneisses	Banded grey, orthogneiss, intermediate to mafic [Canisp Shear fabrics]	Banded grey, orthogneiss, intermediate to mafic [Canisp Shear fabrics]	Banded grey, orthogneiss, intermediate to mafic [Canisp Shear fabrics]	Banded grey, orthogneiss, intermediate to mafic [Canisp Shear fabrics]	High grade intermediate to mafic orthogneisses	High grade intermediate to mafic orthogneisses	High grade intermediate to mafic orthogneisses	Light to dark grey dolerite/granodiorite gneiss, with pegmatite pods.	Light to dark grey dolerite/granodiorite gneiss, with pegmatite pods.	
Structure	Background gneiss outside Canisp Shear zone margin	Assint terrace, Canisp Shear zone margin	Assint terrace, Canisp Shear zone margin	Assint terrace, Canisp Shear zone margin	Assint terrace, Canisp Shear zone margin	Assint terrace, background gneiss fabrics	Assint terrace, background gneiss fabrics	Assint terrace, background gneiss fabrics	Assint terrace, Canisp Shear zone margin	Assint terrace, Canisp Shear zone margin	Assint terrace, Canisp Shear zone margin	Assint terrace, Canisp Shear zone margin	Assint terrace, Canisp Shear zone margin	Assint terrace, Canisp Shear zone margin				
number of fractures	44	43	6	5	6	20	38	38	53	60	60	60	60	60	60	60	60	
length (m)	1.1	1.1	1.1	1.1	1.1	3.25	14.5	14.5	12.738	12.738	12.738	12.738	12.738	12.738	12.738	12.738	12.738	
PL Prob	97.88	72.60	68.88	98.44	0	78.68	98.30	98.30	91.72	98.44	98.40	98.40	98.44	98.44	98.44	98.44	98.44	
PL α	1.4013	1.7352	1.9641	2.1224	1.4657	2.0231	1.3711	2.0763	1.9171	1.9718	1.6109	1.8465	1.9314	2.0763	2.0211	2.0217	2.0217	
uc	0	0	0	0	0	0	0	0	0	0	0	0	0	0	0	0	0	
lc	0	0	0	0	0	0	0	0	0	0	0	0	0	0	0	0	0	
lmin																		
Truncated and censored sample distribution fitting Using MLF approach (see text)																		
LN Prob	99.44	98.20	98.4	98.8	98.24	99.56	99.32	99.2	98.52	99.04	98.24	98.4	98.24	98.24	98.24	98.24	98.24	
LN mu	0.4992	0.1005	0.5187	0.4903	1.5319	0.4907	0.39106	0.49417	0.49417	0.49417	0.4974	0.4974	0.4974	0.4974	0.4974	0.4974	0.4974	
LN sigma	0.80444	0.3293	0.5312	0.5041	0.49571	0.48127	0.72165	0.67445	0.41534	0.47439	0.76437	0.64823	0.67445	0.5115	0.37238	0.47237	0.40224	0.5312
uc	0	10	10	0	20	30	0	0	15	0	15	0	20	45	0	40	0	0
lc	0	0	0	0	0	0	0	0	0	0	0	0	0	80	100	60	100	
lmax	100	90	90	100	80	100	100	85	100	80	75	100	80	55	100	60	100	
Exp prob	98.44	95.52	95.52	95.52	95.52	98.44	98.44	98.44	98.44	98.44	98.44	98.44	98.44	98.44	98.44	98.44	98.44	
Lambda	1.0316	0.54821	1.88881	0.51310	1.3350	1.02041	1.3372	1.3338	2.13350	2.13350	0.86882	0.83996	0.76683	1.0041	0.40303	0.93883	0.63039	1.3724
uc	55	70	85	0	0	0	0	85	85	85	85	85	85	90	0	0	0	0
lc	0	5	0	0	0	0	0	60	5	0	0	0	55	25	0	0	0	100
lmin	45	55	85	0	0	0	0	60	10	15	10	15	10	45	20	75	100	
PL Prob T&C	98.48	98.1	98.12	98.44	99	98.45	99.44	99.44	98.52	98.84	98.84	98.84	98.84	98.84	98.84	98.84	98.84	
PL α	2.3311	2.0278	2.1314	2.1224	2.3741	2.5943	2.00039	0.00053	0.00044	0.00044	0.00083	0.00005	0.0005	0.0005	0.0005	0.0005	0.0005	
uc	0.584	0.51	0.35	0.11	0.217	0.8	0.43	0.5	0.49	0.545	1.32	0.5	0.74	0.67	1.57	0.74	0.78	
lc	0	10	15	0	30	40	15	15	20	25	35	10	15	35	15	35	15	
PL Prob T&C	98.2	98.2	98.4	98.4	98.92	99.04	99.04	99.04	97.96	97.96	94.96	94.96	94.96	94.96	94.96	94.96	94.96	
PL α	1.92	1.92	2.1	1.89	1.89	1.72	1.72	1.72	1.72	1.72	2.3197	2.3197	2.3197	2.3197	2.3197	2.3197	2.3197	
xmin	626	1114	515	515	412	412	793	793	793	793	793	793	793	2075	2075	2075	2075	
lc	5	30	0	0	0	0	0	0	0	0	0	0	0	15	0	0	0	

Clair regional length datasets									
	CL_EW2_L1	CL_NS1_L1	CL_NS2_L1	CL_NW2_L1	CL_NE-SW1_L1	CL_NE-SW2_L12			
Dataset	Clair seismic attribute	n/a	n/a	n/a					
Grid Reference	n/a	n/a	n/a	n/a	n/a	n/a	315	45	45
Transect Orientation	---	---	---	---	---	---	---	---	---
Lithology	Lewisian Gneisses	Lewisian Gneisses	Lewisian Gneisses	Lewisian Gneisses					
Structure	Rona Ridge	Rona Ridge	Rona Ridge	Rona Ridge					
number of fractures	39	30	41	31	49	46			
Length (m)	15 900	14 100	14 300	10 500	24 700	24 000			
PL Prob	97.92	75.6	98.92	99.04	52.36	54.56			
PL α	1.91	1.61	1.89	1.72	1.97	1.66			
uc	0	0	0	0	0	0			
lc	0	0	0	0	0	0			
lmin									
lmax									

Sample No	Sample Area	Total Trace-length	I	Y	X	E	Total	No. Lines	No. Branches	Average Line Length	Avge Branch Length	Connect/line	Connect/branch	Frequency	Intensity
AnB T1b	716743.2549	16881.43844	134	168	21	45	323	151	361	111.80	46.76	2.50	1.63	0.0005	0.024
AnB T2	364893.8289	11509.77525	90	215	68	43	373	152.5	503.5	75.47	22.86	3.71	1.82	0.0014	0.032
AnB T3	785397.5	19634.95408	55	277	28	50	360	166	499	118.28	39.35	3.67	1.89	0.0006	0.025
AnB T4	502654.4	14765.48547	34	238	14	47	286	136	402	108.57	36.73	3.71	1.92	0.0008	0.029
AnB T5	125663.6	6911.503838	31	341	22	44	394	186	571	37.16	12.10	3.90	1.95	0.0045	0.055
AnB T6	785397.5	16100.66235	42	171	8	41	221	106.5	293.5	151.18	54.86	3.36	1.86	0.0004	0.021
AnB T7a	1433720.525	29181.66511	58	360	25	55	443	209	619	139.63	47.14	3.68	1.91	0.0004	0.020
AnB T7b	1433720.525	32895.69522	73	574	61	62	708	323.5	1019.5	101.69	32.27	3.93	1.93	0.0007	0.023
AnB T8	2286419.986	36851.55531	69	280	29	55	378	174.5	512.5	211.18	71.91	3.54	1.87	0.0002	0.016
AnB T9	180523.8104	11672.77364	51	393	32	62	476	222	679	52.58	17.19	3.83	1.92	0.0038	0.065
AnB T10	275979.3576	14432.61802	62	405	20	62	487	233.5	678.5	61.81	21.27	3.64	1.91	0.0025	0.052
Clair 1 a	3061.875173	373.163	6	5	6	14	17	5.5	22.5	67.85	16.59	4.00	1.73	0.0073	0.122
Clair 1 b	3061.875173	402.862	9	17	4	12	30	13	38	30.99	10.60	3.23	1.76	0.0124	0.132
Clair 6	3061.875173	385.464	5	9	3	12	17	7	22	55.07	17.52	3.43	1.77	0.0072	0.126
Clair 1 c	3061.875173	697.436	6	52	6	24	64	29	93	24.05	7.50	4.00	1.94	0.0304	0.228
Clair 1 d	3061.875173	565.945	5	41	1	23	47	23	66	24.61	8.57	3.65	1.92	0.0216	0.185
Clair 2 a	3061.875173	612.268	8	35	7	18	50	21.5	70.5	28.48	8.68	3.91	1.89	0.0230	0.200
Clair 2 b	3061.875173	732.328	6	62	5	20	73	34	106	21.54	6.91	3.94	1.94	0.0346	0.239
Clair 2 c	3061.875173	326.205	6	10	2	5	18	8	22	40.78	14.83	3.00	1.73	0.0072	0.107
Clair2_d	3061.875173	361.948	2	17	0	13	19	9.5	26.5	38.10	13.66	3.58	1.92	0.0087	0.118
RR1	3061.875	679.536	2	39	6	22	47	20.5	71.5	33.15	9.50	4.39	1.97	0.0234	0.222
RR2	3061.875	421.048	5	30	0	17	35	17.5	47.5	24.06	8.86	3.43	1.89	0.0155	0.138
RR3	3061.875	763.406	5	63	6	24	74	34	109	22.45	7.00	4.06	1.95	0.0356	0.249
RR4	3061.875	1078.614	5	173	10	32	188	89	282	12.12	3.82	4.11	1.98	0.0921	0.352
RR5	3061.875	532.007	4	30	0	15	34	17	47	31.29	11.32	3.53	1.91	0.0154	0.174
RR6	3061.875	841.229	20	72	6	26	98	46	130	18.29	6.47	3.39	1.85	0.0425	0.275
Assynt Regional	3.03608E+13	188445192.4	246	194	161	82	601	220	736.00	856569.06	256039.66	3.23	1.67	0.0000	0.000